# Coordinated Mapping of $Li^+$ Flux and Electron Transfer Reactivity during Solid-Electrolyte Interphase Formation at a Graphene Electrode

Zachary T. Gossage,[a] Jingshu Hui,[a] Dipobrato Sarbapalli[b] and Joaquín Rodríguez-López*[a]

[a] Department of Chemistry, University of Illinois at Urbana−Champaign, 600 S Mathews Ave., Urbana, Illinois 61801, United States
[b] Department of Materials Science and Engineering, University of Illinois at Urbana-Champaign, 1304 W Green St., Urbana, Illinois 61801, United States

**Corresponding Author**
*To whom all correspondence should be addressed:
Prof. Rodríguez-López: joaquinr@illinois.edu (Email) and 217-300-7354 (Phone).

# Table of Contents page

## Section 1: Supplemental Figures

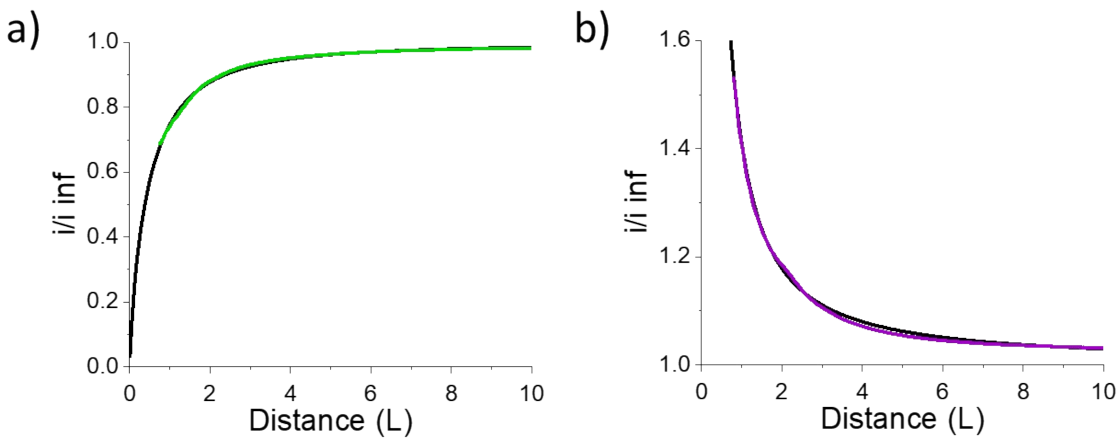

**Figure S1**. Approach curves to MLG with HgDWs before single spot measurements of Li$^+$ flux during SEI formation. a) Approach curve to $SiO_2$ region using the HgDW before measurement at MLG (Figure 2, main text). b) Approach curve to MLG before using the HgDW for measurements above the $SiO_2$ (Figure 2, main text).

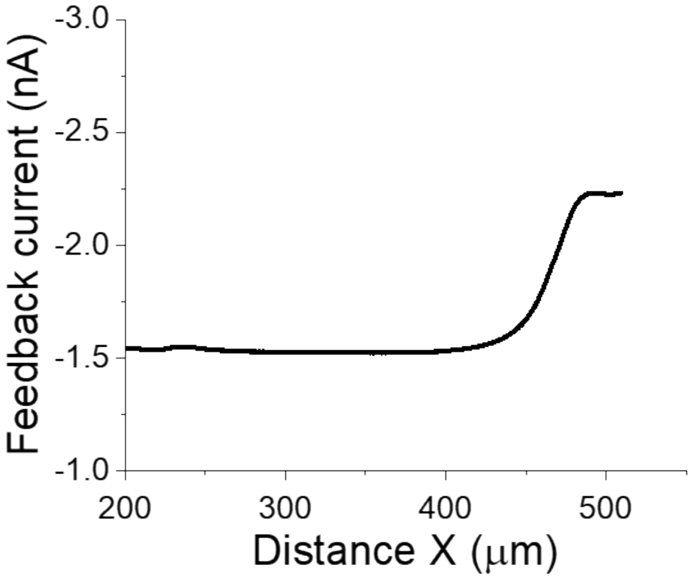

**Figure S2**. Positioning of HgDW above the MLG surface for SEI formation measurement (Figure 2, main text). The probe was retracted -50 µm in the X direction after finishing the scan.

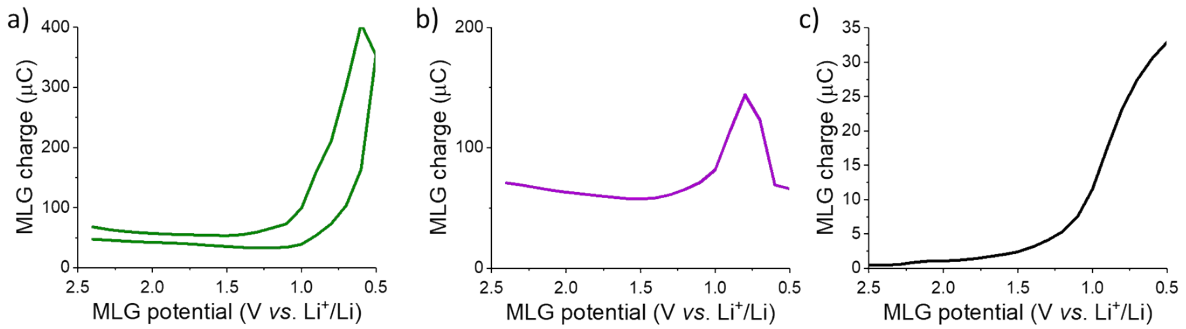

**Figure S3**. Integrated response of MLG during *in situ* SEI formation measurements. a) Full cycle of SEI formation for MLG used in MLG measurement. b) Response of MLG sample used in $SiO_2$ measurement. c) Response on another MLG sample during *in situ* SEI formation.

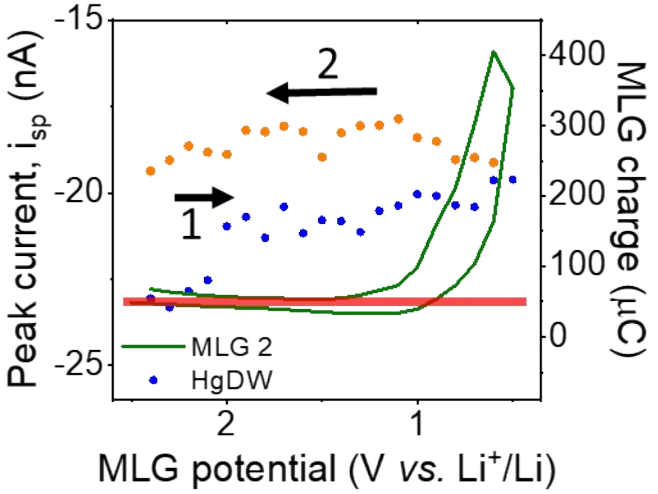

**Figure S4**. HgDW response at MLG during forward and reverse sweeps while forming the SEI.

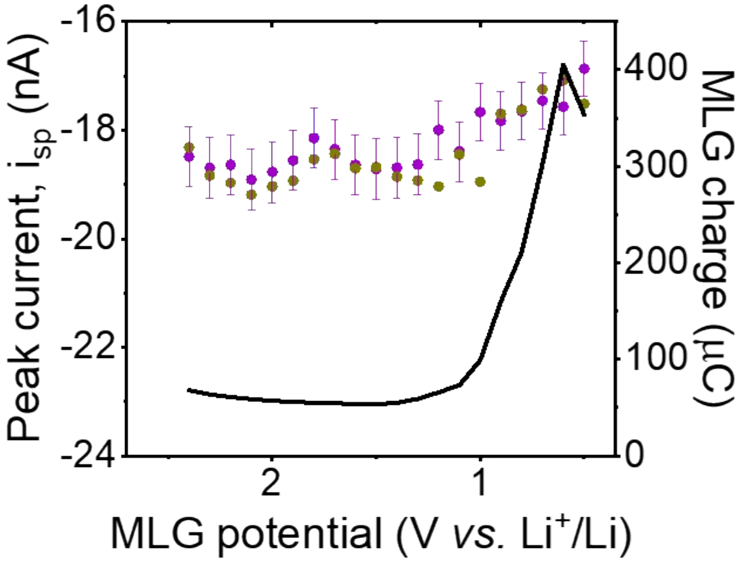

**Figure S5**. Comparison of $i_{sp}$ measured at different times with the HgDW above $SiO_2$ during potential steps at an MLG substrate while forming the SEI. The gold and purple curves were measured at ~5 s and ~15 s after each new potential was applied, respectively.

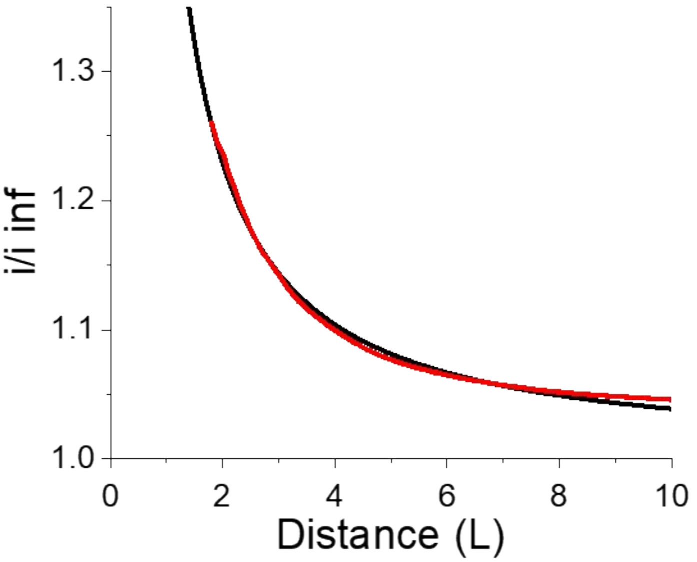

**Figure S6**. Approach curves to MLG with HgDW before linescan during SEI formation (Figure 3, main text).

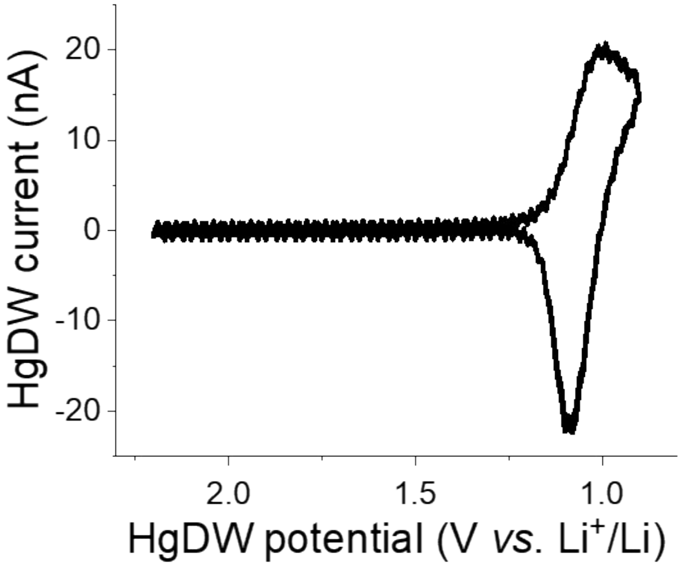

**Figure S7**. Cycling of the HgDW before applying potentials at MLG to acquire a line scan during pulsed SEI formation.

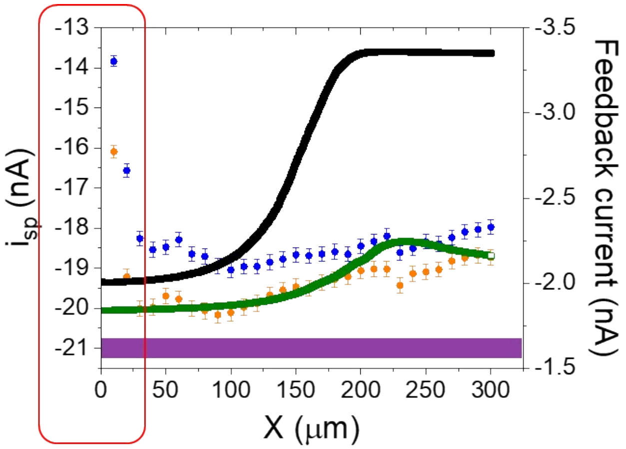

**Figure S8**. Response of the HgDW during initial pulses at MLG while acquiring a line scan profile of $Li^+$ consumption during SEI formation.

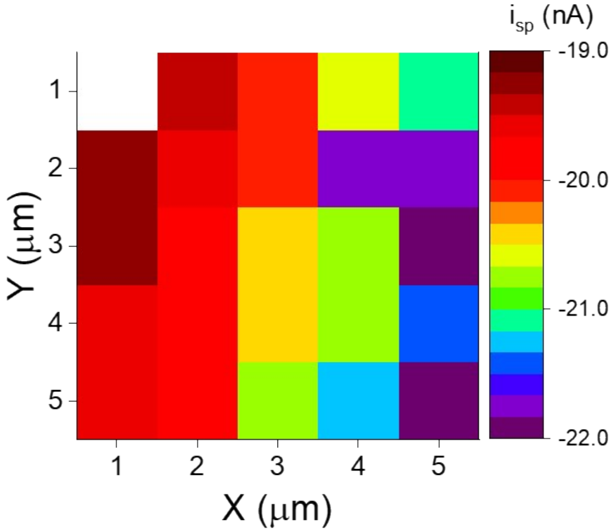

**Figure S9**. $Li^+$ flux map during anodic pulses (1.8 V vs. $Li^+/Li$) for deintercalation.

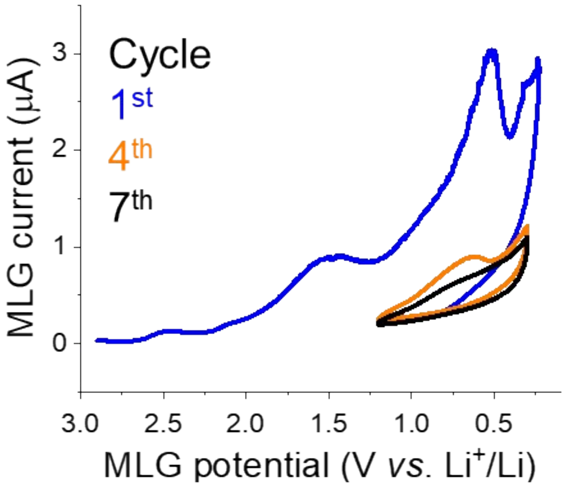

**Figure S10**. SEI formation at the MLG substrate using voltammetry in 0.1 M $LiBF_4$.

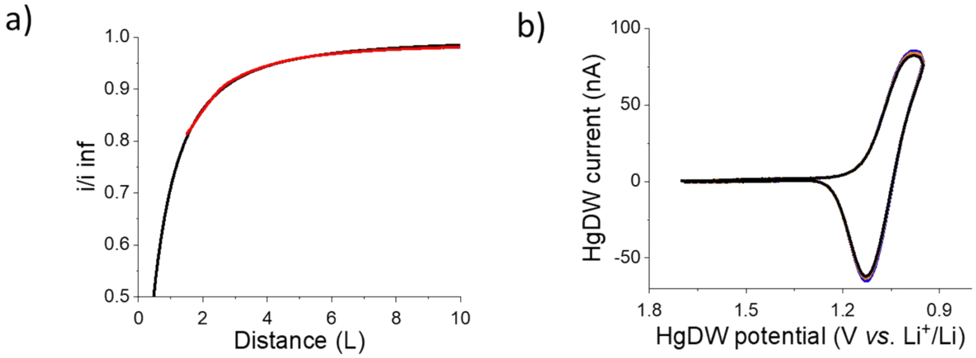

**Figure S11**. Approach and cycling of HgDW before $Li^+$ flux measurement at a preformed SEI. a) Approach curve to $SiO_2$ before positioning. b) Cycling of the HgDW with $Li^+$.

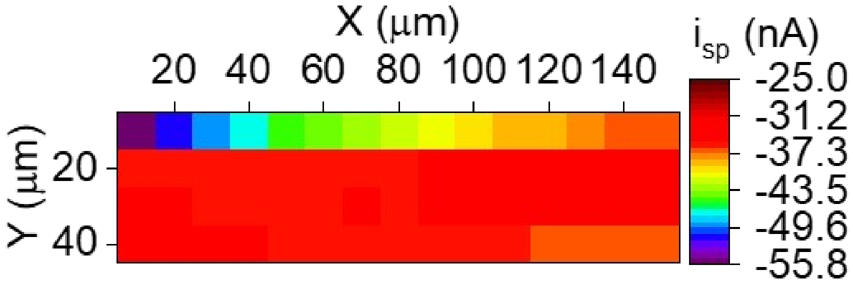

**Figure S12**. Initial response during Li$^+$ flux mapping for cathodic pulses (0.06 V vs. Li/Li$^+$) at a preformed SEI.

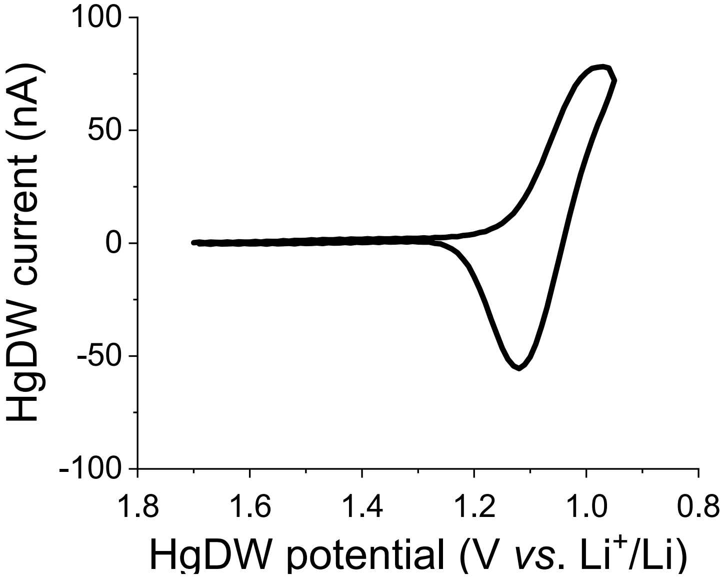

**Figure S13**. CV of HgDW after positioning and before imaging of Li$^+$ flux at a preformed SEI on MLG.

## Section 2: COMSOL Simulations

We conducted simulations using the Transport of Diluted Species module within COMSOL Multiphysics 4.4, and Fick's laws for diffusion. We explored the impact of a single negative pulse (related to Figure 3, main text) and diffusional broadening at the MLG-$SiO_2$ edge on Li$^+$ flux measurements (Figure 4, main text). We used a 2D geometry representing a cross section of the HgDW probe positioned near the MLG electrode (Figure S14). Three active regions were defined: 1) Amalgam, 2) MLG, and 3) Solution. All parameters used in the simulations are listed in Supplemental Table 1 and referenced appropriately. At the Amalgam domain and its Flux boundary with the Solution domain, Li$^+$ was consumed to produce reduced species (M(Hg)) that could diffuse freely into the Amalgam domain. The simulated probe response and associated Li$^+$ flux was controlled via Butler-Volmer to approximate an amalgamation/stripping voltammogram. The MLG domain was controlled as another Flux boundary defined to consume $Li^+$ at a diffusion limited rate. Open boundaries were set to bulk conditions.

**Supplemental Table S1**. Parameters for COMSOL simulations.

| Parameter | Variable | Simulated value | Reported values |
|---|---|---|---|
| MLG length | MLGL | 200 x $10^{-6}$ [m] | - |
| MLG and SEI height | MLGH | 100 x $10^{-9}$ [m] | - |
| Solution height | SH | 500 x $10^{-6}$ [m] | - |
| Solution length | SL | 500 x $10^{-6}$ [m] | - |
| Glass height | GH | 2 x $10^{-6}$ [m] | - |
| Glass length | GL | 500 x $10^{-6}$ [m] | - |
| HgDW electrode radius | a | 12.5 x $10^{-6}$ [m] | - |
| HgDW height | PH | 500 x $10^{-6}$ [m] | - |
| Ratio of glass to electrode radius | RG | 3.0 | - |
| Bulk $Li^+$ concentration | ox0 | 0.01 [mol] | - |
| Probe-substrate distance | d | 12.5 x $10^{-6}$ [m] | - |
| $Li^+$ diffusion coefficient in PC | Lid | 1.7 x $10^{-10}$ [$m^2$/s] | 1.7,[1] 2.4[2] for PC |
| $Li^+$ diffusion coefficient in Hg amalgam | LHg | 5.0 x $10^{-10}$ [$m^2$/s] | 9.2[3] |
| HgDW scan rate | nu | 1.0 [V/s] | - |
| Potential sampling interval | Eint | 0.01 [V] | - |
| Time sampling interval | tinit | 0.01 [s] | - |
| Oxidative potential limit (HgDW scan) | Eox | 2.0 [V] | - |
| Reductive potential limit (HgDW scan) | Ered | 0.6 [V] | - |
| Reduction potential - $M^+$ -> M(Hg) | $E^0$ | 0.96 [V] | - |
| Apparent rate constant - $M^+$ -> M(Hg) | $k^0$ | 0.0005 [cm/s] | 0.008,[1] 0.0005[4] |
| Forward rate constant – HgDW | $k_f$ | **See reference 4** | - |
| Backward rate constant – HgDW | $k_b$ | **See reference 4** | - |
| Etch depth | etch | 12.5 x $10^{-6}$ [m] | - |
| Transfer coefficient for Hg-HgLi | $\alpha$ | 0.5 | 0.7[2] |
| Moles of electrons per mole $M^+$ reduction | $n$ | 1 | - |
| Faraday's constant | F | 96485.3 [C/mol] | - |
| Universal gas constant | R | 8.314 [J/(mol * K)] | - |
| Temperature | T | 298.15 [K] | - |
| F/(R*T) | $f$ | 38.9 [1/V] | - |

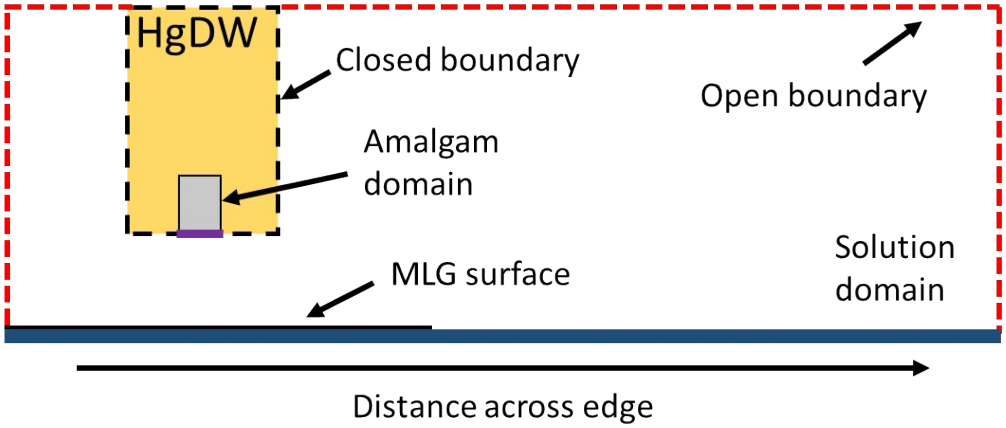

**Figure S14**. 2D geometry used in COMSOL model for evaluating edge and pulse effects. The probe was translated across the edge to evaluate location-dependent impact on the probe response.

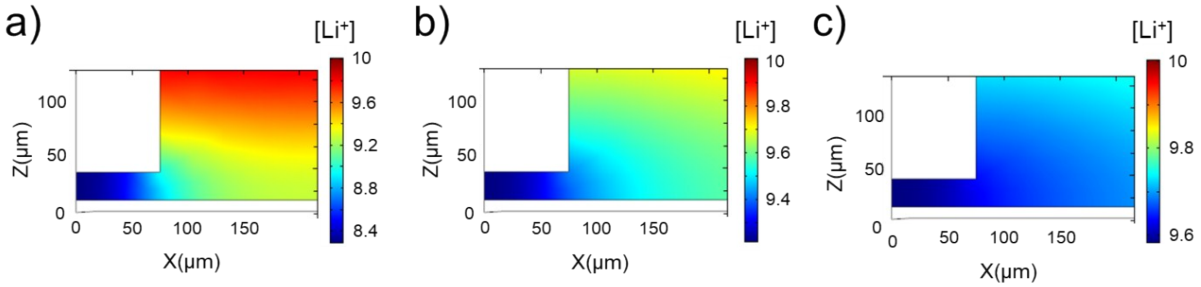

**Figure S15**. Simulation result of a 60 s negative pulse at an MLG substrate and nearby SECM probe. a) $Li^+$ concentration gradient between the modeled probe and substrate 14 s after a negative pulse (60 s) to consume $Li^+$ at a diffusion-limited rate. b) The remaining $Li^+$ concentration gradient between the probe and MLG after 60 s. c) 120 s after the pulse.

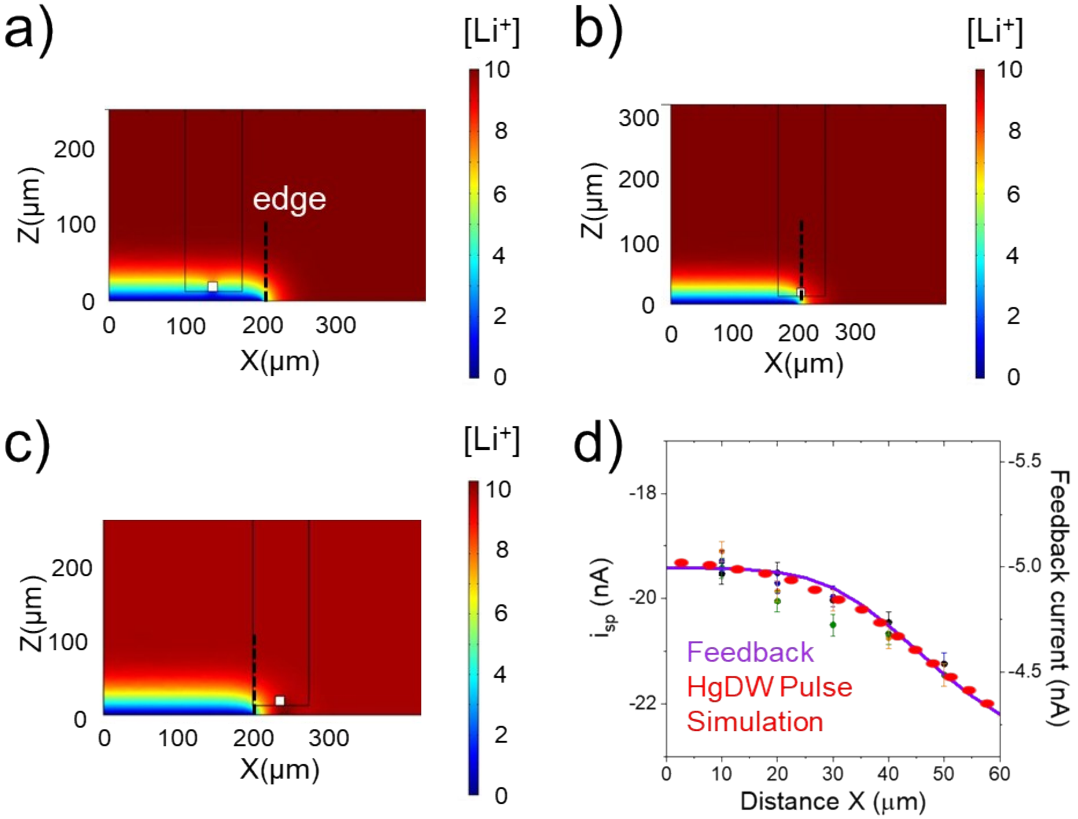

**Figure S16**. Simulations of $i_{sp}$ with the SECM probe at different MLG locations during pulsing. Final result of simulation with the HgDW at a) 140, b) 200, and c) 230 µm. For reference, the MLG ends at 200 µm. d) Simulated $i_{sp}$ across the edge normalized to the experimental $i_{sp}$.

[1] C. Cronnolly, K. C. Pillai, W. E. Waghorne, *J. Electroanalytical chemistry and interfacial electrochemistry*. **1986**, *207*, 177-187.
[2] G. J. Hills, L. M. Peter, *Journal of Electroanalytical Chemistry and Interfacial Electrochemistry*. **1974**, *50*, 175-185.
[3] L. F. Kozin, S. C. Hansen, Mercury handbook: chemistry, applications and environmental impact, Royal Society of Chemistry, **2013**.

[4] Z. T. Gossage, J. Hui, Y. Zeng, H. Flores-Zuleta, J. Rodríguez-López, *Chemical Science*. **2019,** *10*, 10749-10754.